Conference paper

Francesco Papi, Giulia Targetti, Linda Cerofolini, Claudio Luchinat, Marco Fragai and Cristina Nativi*

Nanoparticles for the multivalent presentation of a TnThr mimetic and as tool for solid state NMR coating investigation

https://doi.org/10.1515/pac-2019-0210

Abstract: The fully characterization of tumor associated antigens (TAAs) and of tumor associated carbohydrate antigens (TACAs) have opened the avenue of cancer immunotherapy. The intrinsic poor immunogenicity of TACAs, however, spotlighted the importance of multivalent presentation of the antigen(s) to trigger an immune response. Nanoparticles are excellent scaffolds for this purpose. Here we reported on the easy glycosylation of iron-based and biocompatible dextran-based nanoparticles with **1**, a mimetic of the TnThr antigen. The multivalent presentation of **1** induced the induction of TNF-α and IL-6/IL10, respectively. The multivalent glycosylation of silica nanoparticles (GSiNPs) was also performed and saccharide loading qualitative assessed by solid state NMR. Our results offer the proof of concept that biomolecules coating can also be investigated on solid system by NMR.

Keywords: dextran-based nanoparticles; glycosides; ICS-29; iron oxide nanoparticles; multivalency; nanoparticles; silica nanoparticles; tumor associated carbohydrate antigens.

Introduction

A plethora of tumors present on their surface characteristic glycosyl patterns, different from those found on normal cells and often correlated with tumors' type and stage [1]. These tumor antigenic determinants, known as tumor associated carbohydrate antigens (TACAs), are intrinsically poor immunogens [2] and their use to trigger an effective activation of tumor bearing hosts' immune system requires specific strategies which have been and still are a challenge.

Taking inspiration from Nature, a successful workaround to face the low immunogenicity of TACAs is represented by their multivalent display artificially obtained by their coupling onto multivalent scaffolds [3]. A great deal of natural and synthetic scaffolds have been proposed for the multivalent presentation of selected epitopes to the immune system. Among them proteins [4], dendrimers [5], silica and gold nanoparticles [3] likely are the most used, but also magnetic iron oxide nanoparticles [6], attracting for the applications

Article note: A collection of invited papers based on presentations at the 29th International Carbohydrate Symposium (ICS-29), held in the University of Lisbon, Portugal, 14–19 July 2018.

***Corresponding author: Cristina Nativi,** Dipartimento di Chimica, University of Florence, via della Lastruccia, 3,13 – 50019 Sesto F.no (FI), Italy, e-mail: cristina.nativi@unifi.it. https://orcid.org/0000-0002-6312-3230
Francesco Papi and Giulia Targetti: Dipartimento di Chimica, University of Florence, via della Lastruccia, 3,13 – 50019 Sesto F.no (FI), Italy
Linda Cerofolini: CERM, University of Florence, via L. Sacconi, 6 – 50019 Sesto F.no (FI), Italy
Claudio Luchinat and Marco Fragai: Dipartimento di Chimica, University of Florence, via della Lastruccia, 3,13 – 50019 Sesto F.no (FI), Italy; and CERM, University of Florence, via L. Sacconi, 6 – 50019 Sesto F.no (FI), Italy

© 2019 IUPAC & De Gruyter. This work is licensed under a Creative Commons Attribution-NonCommercial-NoDerivatives 4.0 International License. For more information, please visit: http://creativecommons.org/licenses/by-nc-nd/4.0/

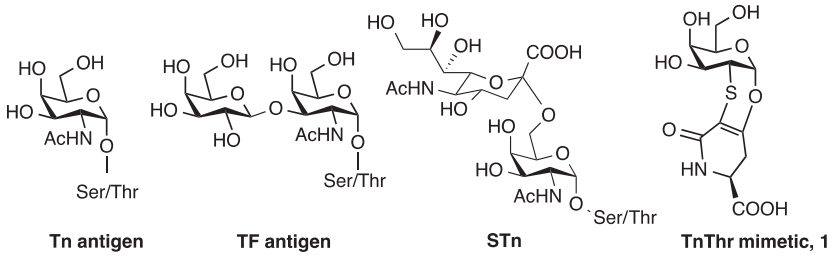

Fig. 1: Structure of tumor antigens Tn, TF, STn and STF and of TnThr mimetic **1**.

they offer in tumor monitoring, and polymeric biocompatible nanoparticles [7] are largely studied for nanomedicine-based therapies.

Some years ago, we designed and synthesized a mimetic of the glycoaminoacid ThThr, a TACA largely expressed by cancer mucins. Mucins are heavily O-glycosylated extracellular proteins which are the major component of the protective biofilm surrounding organs. Normal mucins are characterized by highly branched oligosaccharides, glycosylated through a serine (Ser) or a threonine (Thr) residue to repetitive peptide motifs while in cancer mucins an oversimplification occurs. As consequence, mono-, di- and trisaccharides normally hidden, become exposed to the immune system. These simple saccharides, namely α-Tn (or Tn), TF (or T) and STn have been proved mucin-associated antigens and their level of expression has been correlated with the stage of the tumor and with its tendency to produce metastasis [8] (Fig. 1).

The Tn antigen is the most studied among the mucin-related antigens [8]. Recently, it has been demonstrated that antigenicity is influenced by the different presentation of the GalNAc moiety to the immune system produced by the residue of Thr with respect to the residue of Ser. As a matter of fact, if the GalNAc is linked to a Thr residue, the Thr methyl group causes an important alteration on the 3D-orientation of the sugar as well as on the surrounding water shell [9]. Keeping this in mind, the TnThr mimetic **1** (Fig. 1), preserves this 3D-orientation and is well recognized by lectins which selectively bind galactose residues [10]. Moreover, mimetic **1** when linked to suitable adjuvants, is able to elicit a specific immune response in a breast cancer animal model [11]. In order to increase the immunogenicity of the TnThr mimetic **1**, we also took advantage from multivalent nanoscaffolds and in particular we prepared three different glycosyl nanosystems: (a) ferrimagnetic iron oxide nanoparticles [12], (b) biocompatible single-chain polymer nanoparticles [13] and silica nanoparticles.

Iron nanoparticles

In the case of ferromagnetic iron oxide nanoparticles (MNPs), magnetite/maghemite MNPs with an average diameter of 11 nm were prepared. To decorate the MNPs with **1**, the compound **2** was synthesized (Scheme 1). Derivative **2** presents an hexaethylene glyco-linker with a terminal phosphonate group suitable for the grafting of the TnThr mimetic moiety to MNPs [12].

The glycosyl MNPs obtained (GMNPs) were studied in terms of structural, magnetic and hyperthermic properties, confirming the desired anchoring of **2**. In addition, it was proved that the inorganic cores owned proper magnetic characteristic to be developed for potential clinical applications as heat mediators in the magnetic fluid hyperthermia [12]. The absence of toxicity of MNPs and GMNPs was also tested. After purity evaluation of MNPs and GMNPs to exclude endotoxin contaminations, the effects of GMNPs on immune cells were studied. Macrophages are powerful immune cells inducing an immediate response against harmful species and acting as antigen presenting cells (APCs) to trigger an adaptive immune response. To investigate the effects of non-self antigen decorated GMNPs as immunomodulators, mouse monocyte/macrophage quiescent cell line (RAW 264.7) as model of human macrophages were treated with GMNPs and with two negative controls that is: glucosylated MNPs (GlcMNPs) and polyethylene glycol MNPs (PEMNPs) [12]. The cell viability and qualitative cellular uptake (Prussian blue staining) of GMNPs and GlcMNPs in comparison with

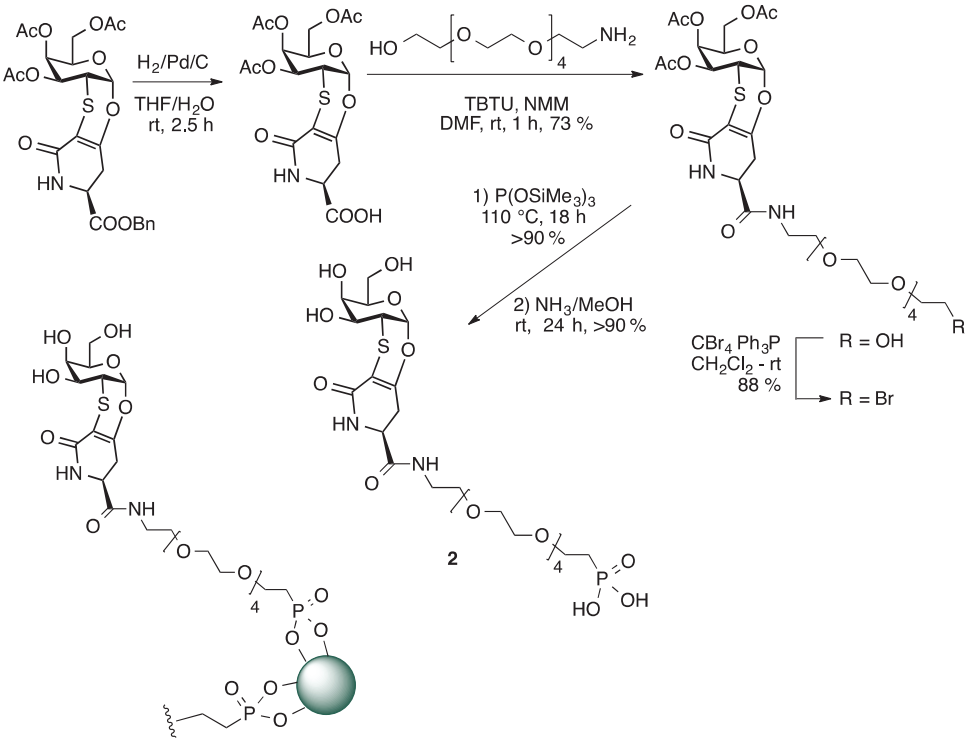

Scheme 1: Synthesis of compound **2** and representation of glycosylated MNPs.

non-functionalized citrate coated MNPs (CMNPs), PEMNPs and with the monovalent TnThr mimetic **2** were evaluated. All compounds tested were biocompatible, in addition, the typical Prussian blue staining images of cells showed that MNPs, either glycosylated (GMNPs and GlcMNPs) or not (citrate coated, CMNPs) are able to enter into macrophages. Of note, PEMNPs were not endocyted while mimetic **2**, which was not graphed to MNPs is not visible with this method. Quantitatively, the endocytoses of **2**, CMNPs, PEMNPs, GMNPs and GlcMNPs were assessed by flow cytometry (FACS) [12]. The side-scattered light (SSC) intensity, used as indicator of particle uptake, increased after cell treatment with MNPs, either functionalized or not, because the cell granularity was enhanced. A similar level of cellular uptake was observed with glycosylated MNPs (GMNPs and GlsMNPs), conversely the SSC intensity did not change upon cells exposure to PEMNPs or TnThr mimetic **2**. The investigation of the effector functions triggered by glycosylated MNPs on the same cells was also performed. Remarkably, looking at the production of the typical pro-inflammatory mediator (TNF-α), a time dependent TNF-α gene expression and protein release at levels comparable to the golden standard lipopolysaccharides (LPS, 0.1 μg/L) was detected. In the case of GlcMNPs only a 50 % of the TNF-α increasing was induced in a time-independent way. Our data clearly showed the biological role in cellular uptake of the monosaccharides used for the coating of MNPs and demonstrated that a multivalent display of the TnThr mimetic is required for macrophage activation (see Supporting Information).

Dextran-based single chain polymer nanoparticles

Aware of the main concerns affecting metal nanoparticles as in vivo delivery systems [14], we were attracted by biocompatible/biodegradable single-chain polymer nanoparticles (SCPNs) as nanocarriers [15]. SCPNs have soft matter characteristics, small and controllable size and shape. In particular, to obtain water-dispersible SCPNs, we took advantage from the reported synthesis and functionalization of dextran-based single chain polymer nanoparticles (DXT-SCPNs) [16] for an efficient presentation and local concentration of the TnThr mimetic **1**. For the decoration of DXT-SCPNs the derivative **3** was synthesized by the coupling of **1a** to

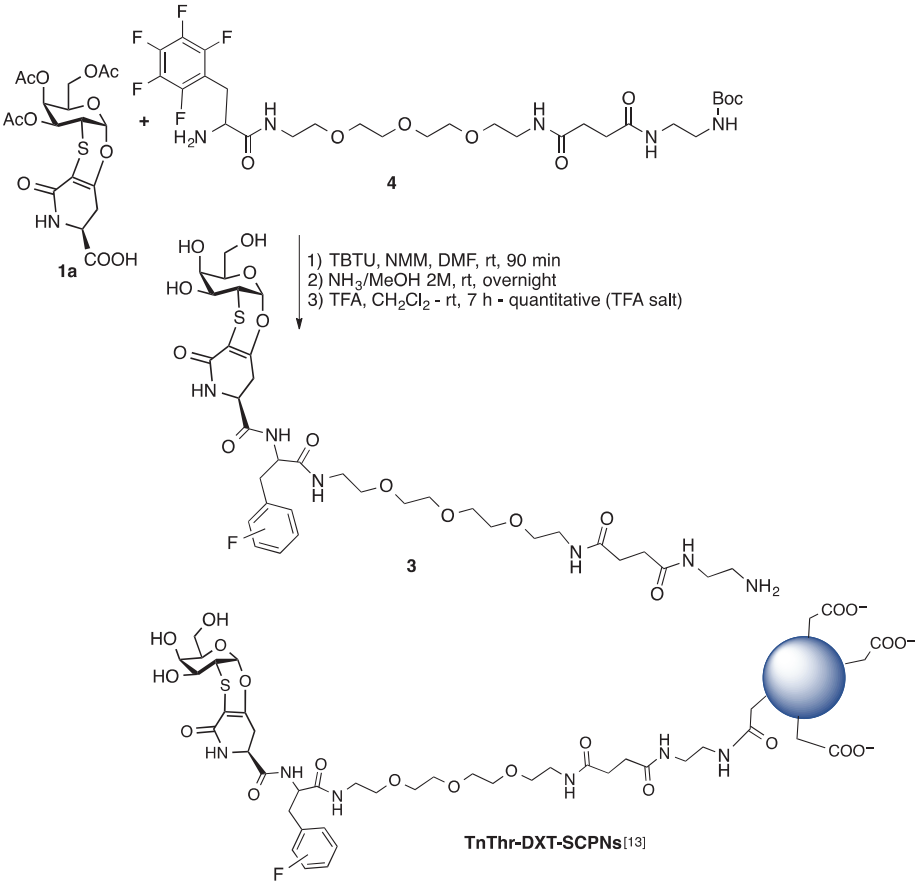

Scheme 2: Synthesis of mimetic **3** and representation of TnThr-DXT-SCPNs.

the fluorinated spacer **4** as depicted in Scheme 2. The NBoc-protecting group shall be removed just before nanoparticles decoration (Scheme 2).

The covalent coupling of the TnThr mimetic amido-derivative **3** with DXT-SCPNs was run under condensation standard conditions (EDC, DMAP, DMSO, rt, 16 h). After purification the TnThr-DXT-SCPNs were freeze-dried, re-dispersed in aqueous buffer (PBS, pH 7.4) and fully characterized [13]. DXT-SCPNs and TnThr-DXT-SCPNs (average diameter 42 nm) were then tested to prove the absence of toxicity and of endotoxin contamination [13].

Innate immune response was also studied for the multivalent display of the TnThr mimetic **2** linked onto DXT-SCPNs (TnThr-DXT-SCPNs). In this case, we observed that the stimulation of human PBMC (isolated from healthy donors) with TnThr-DXT-SCPNs triggered the secretion of IL-6 and IL-10, similarly as the positive control LPS and as already reported for mucin glycoproteins [17]. Conversely, non-glycosylated DXT-SCPNs induced nor IL-6 or IL-10 secretion (see Supporting Information).

Silica nanoparticles

Silica nanoparticles (SiNPs) are easy to prepare, non-expensive, characterized by adsorption and encapsulation capacity. Although widely used in the biomedical field, SiNPs biocompatibility was recently matter of concern [18]. As a matter of fact, SiNPs interact with the immune system and induce immunotoxicity. However, the toxicity of SiNPs depends on nanoparticles physical and chemical properties and on the immune cells type, and to date no adequate studies properly address this scientific and social problem [18].

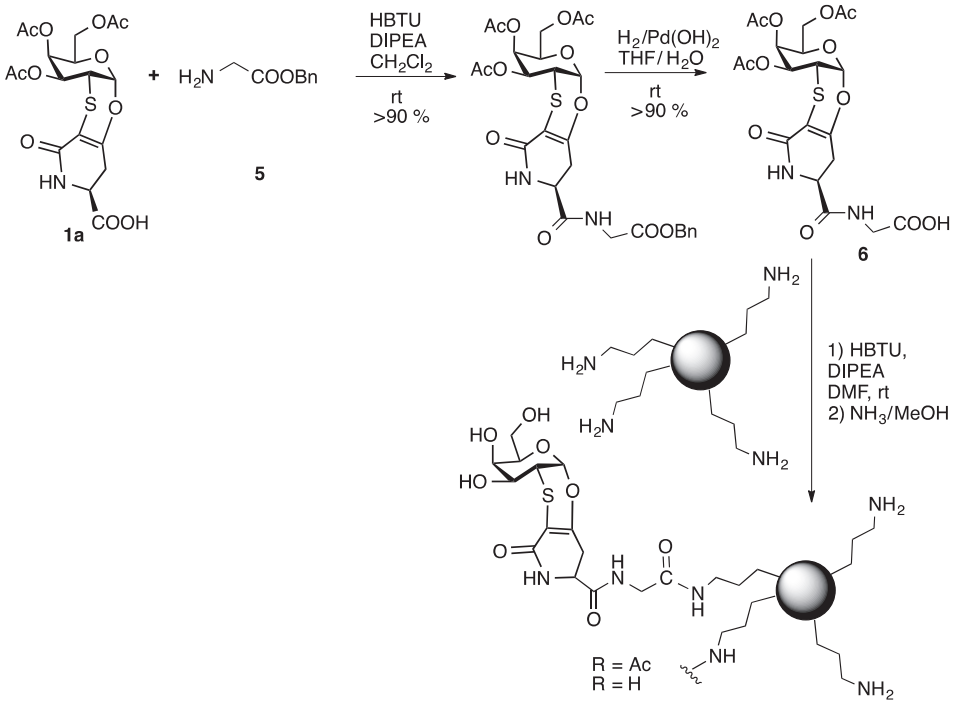

Scheme 3: Synthesis of glycosylated SiNPs.

In this context, recent developments in biomolecular solid state NMR (SSNMR) have demonstrated that SSNMR is a powerful tool for the characterization of hybrid inorganic-biomolecular composites [19–26]. With this in mind, we reasoned that it could be possible to take advantage from SiNPs for the multivalent presentation of the TnThr mimetic **1** and for the SSNMR characterization of the glycosyl-nanosystem obtained. Solution NMR experiments are usually inefficient to characterize molecules covalently bound on the surface of nanoparticles due to the fast transverse relaxation rate that broaden the signals beyond the detection threshold. Conversely, ^{1}H–^{13}C cross polarization (CP) spectra under magic angle spinning (MAS) conditions do not suffer from molecular-weight limitations, although sensitivity and resolution can be limited for samples with natural abundance.

In this study we selected commercially available SiNPs presenting an organic coating. In particular SiNPs coated with aminopropyl chains were chosen because the suspected toxic effects of SiNPs are dramatically attenuated by surface-functionalization with amino groups [27], in addition, the terminal amino group can be conveniently used to form an amidic linkage with the TnThr mimetic suitably functionalized with a spacer presenting an activated carboxylic group. In detail, mimetic **1a** was reacted with glycine benzyl ester **5** to give after debenzylation, the amido-derivative **6** which was covalently graphed to the propylamine-coated SiNPs. The functionalized SiNPS were filtered on gooch and washed with DMF and dichlorometane. The subsequent deacetylation was performed on solid phase with ammonia in methanol (4M); after filtration the unreacted species were removed by washing the nanoparticles with methanol to afford the desired glycosylated GSiNPs (Scheme 3).

The original size of the SiNPs did not increase significantly upon glycosylation as estimated by modelling the residue **6** (1.5 nm maximum length), linked to the amino propyl chains coating the silica particles. The loading of GSiNPs was qualitatively investigated by SSNMR. $\{^{1}H\}$-^{13}C CP MAS spectra were collected in isotopic natural abundance on: (i) propylamine-coated SiNPs (Fig. 2, panel a), (ii) acetylated glycosylated SiNPs (Fig. 2, panel b), and (iii) deacetylated glycosylated SiNPs (Fig. 2, panel c). Signals of carbonyl, anomeric and ethylene carbons were observed only on the spectra of the glycosylated silica nanoparticles (Fig. 2, panel b, c), proving the successful grafting of the TnThr mimetic onto SiNPs. Interestingly, the decrease in signal intensity observed in the spectrum of the deacetylated GSiNPs for the signals of carbonyl and methyl carbon atoms, but not for those of the anomeric and ethylene carbons, proves the successful deacetylation of the TnThr mimetic.

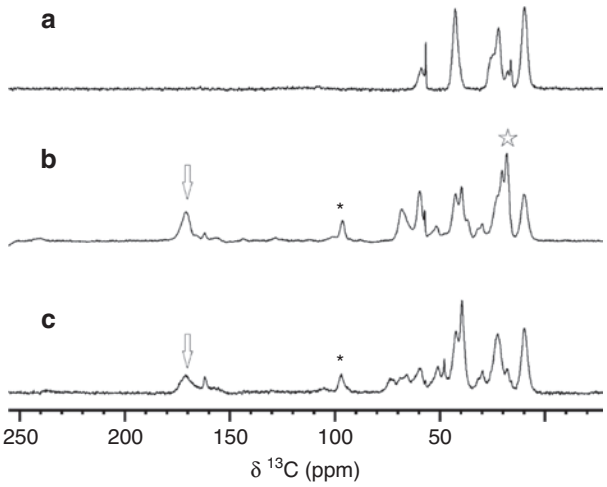

Fig. 2: {^{1}H}-^{13}C CP MAS spectra of (a) propylamine-coated SiNPs, (b) acetylated glycosylated SiNPs and (c) deacetylated glycosylated SiNPs in 3.2 mm rotors, collected on 850 and 800 MHz spectrometers at ~280 K and MAS of 14 kHz. The carbonyl, anomeric, ethylene and methyl signals are marked with arrows, asterisks, and stars, respectively. Of note, the ethylene and anomeric carbons (marked with asterisk) are superimposed.

Conclusions

In conclusion, we reported on the easy glycosylation of three different nanoscaffolds: iron oxide nanoparticles (MNPs), dextran-based single chain polymer nanoparticles (DXT-SCPNs) and silica nanoparticles (SiNPs), with the immunogenic TnThr mimetic **1**. As it happens in Nature, the multivalent presentation of antigenic constructs to the immune system is mandatory to induce an efficient immune-stimulation and a robust immune response. Nanoparticles are ideal tools to this purpose. Thanks to the versatility of the TnThr mimetic structure, to ensure a properly exposure of the antigen, we successfully inserted spacers of different length and polarity between the mimetic and the nanoscaffolds and performed the glycosylation of the nanoparticles relying on different functional groups. In particular, a phosphonate group was chosen for the graphing to MNPs, a primary amino residue was reacted with the carboxylic functions displayed by DXT-SCPNs and a carboxylic group was condensed to the primary $-NH_2$ of the propylamine-coated SiNPs. The glycosylated MNPs (GMNPs) and DXT-SCPNs (TnThr-DXT-SCPNs) were tested in vitro. The monocyte/macrophage and PBMC stimulation observed for the multivalent, with respect to the monovalent, TnThr presentation, confirmed the role of these nanoplatforms in mediating immune recognition.

Finally, glycosylated SiNPs (GSiNPs) were screened by {^{1}H}-^{13}C CP MAS spectra to prove the successful grafting of the nanoparticles. The results provide new perspectives for the use of SSNMR in the characterization of conjugated nano-vaccines and biomolecules-coated nanoparticles.

Experimental section

Materials and methods

Reagents were purchased from commercial suppliers and used without purification. Solution NMR experiment were performed on Bruker Avance II 500 MHz, the spectra were collected at ~298 K. SSNMR experiments were performed on propylamine-coated SiNPs, acetylated glycosylated SiNPs and deacetylated glycosylated SiNPs. The samples were packed in 3.2 mm zirconia rotors. The {^{1}H}-^{13}C CP MAS spectra were recorded using the standard pulse sequence and parameters reported in literature. The spectra were collected at ~280 K on a Bruker Avance III 850 MHz wide-bore spectrometer (213.6 MHz ^{13}C Larmor frequency), equipped with

3.2 mm DVT MAS probe head in triple-resonance mode and on a Bruker Avance III 800 MHz narrow-bore spectrometer (201.2 MHz ^{13}C Larmor frequency) equipped with Bruker 3.2 mm Efree NCH probe-head, under MAS conditions of 14 kHz. ESI-MS mass spectra were recorded on a LCQ-Fleet Ion Trap equipped with a standard Ion spray interface from Thermo Scientific. $[\alpha]^D$ values were measured using a JASCO DIP-370 instrument.

Synthesis of compound 6

TnThr mimetic **1a** (140 mg, 0.31 mmol) was suspended in dry CH_2Cl_2 (3 mL), HBTU (174 mg, 0.46 mmol), DIPEA (89 µL, 0.93 mmol) and glycine derivative, **5** (61 mg, 0.37 mmol) were added and the suspension was stirred at rt for 4 h. After complete conversion (tlc monitoring), the mixture was diluted with CH_2Cl_2 and washed with HCl 1M (×3). The organic layer was dried over Na_2SO_4 and concentrated under vacuum. The crude was purified by flash chromatography (CH_2Cl_2/MeOH 95:5) to give the corresponding amido benzyl ester as white solid (168 mg, 91 %). $[\alpha]_D^{26}$ = +126.5 (c 0.001, CD_3OD); ESI-MS m/z (%): 629.33 (100) $[M+Na]^+$, 1235.08 (97) $[2M+Na]^+$; ^1H NMR (500 MHz, $CDCl_3$) δ: 7.39–7.30 (m, 5H, Ar), 6.98 (t, 1H, J_{NH,CH_2Gly} 5.6 Hz, NH), 6.56 (d, 1H, $J_{NH,H\text{-}5'}$ 3.2 Hz, NH), 5.69 (d, $J_{1,2}$ = 2.7 Hz, 1H, H-1), 5.42 (dd, $J_{4,3}$ = 3.1 Hz, $J_{4,5}$ = 1.1 Hz, 1H, H-4), 5.16–5.15 (m, 2H, CH_2Ph), 5.02 (dd, $J_{3,2}$ = 11.7 Hz, $J_{3,4}$ = 3.1 Hz, 1H, H-3), 4.46–4.41 (m, 1H, H-5), 4.24–4.20 (m, 1H, H-5′), 4.17–4.13 (m, 2H, H-6a, H-6b), 4.12–4.08 (m, 2H, CH_2, Gly), 3.60 (dd, $J_{2,1}$ = 2.7 Hz, $J_{2,3}$ = 11.7 Hz, 1H, H-2), 3.01–2.88 (m, H-4′a, H-4′b), 2.16 (s, 3H, $COCH_3$), 2.07 (s, 3H, $COCH_3$), 2.02 (s, 3H, $COCH_3$); ^{13}C NMR (125 MHz, $CDCl_3$) δ: 170.6 (Cq, CO), 170.2 (Cq, CO), 170.1 (Cq, CO), 170.0 (Cq, CO), 169.5 (Cq, CO), 164.8 (Cq, CO), 155.0 (Cq), 135.22 (Cq, Ar), 128.8 (CH, Ar), 128.7 (Cq, Ar), 128.5 (CH, Ar), 97.3 (Cq), 96.0 (CH, C-1), 69.1 (CH, C-5), 67.6 (CH_2, CH_2Ph), 67.2 (CH, C-4), 66.1 (CH, C-3), 61.7 (CH_2, C-6), 52.4 (CH, C-5′), 41.6 (CH_2, Gly), 36.6 (CH, C-2), 30.9 (CH_2, C-4′), 20.8–20.7 ($3CH_3$, Ac). To a solution of amido benzyl ester (160 mg, 0.26 mmol) in THF/H_2O 100:1 (3 mL), $Pd(OH)_2$/C (20 wt. %, 30 mg) was added. The reaction was stirred at rt for 16 h under H_2 atmosphere, diluted with EtOAc and filtered over a pad of Celite®. The filtrate was concentrated to dryness to give **6** (130 mg, >96 %) as a white solid. $[\alpha]_D^{26}$ = +96.9 (c 0.0035, CH_3OD); ESI-MS *m/z* (%): 515.50 (100) $[M-H]^-$, 1031.33 (50) $[2M-H]^-$; ^1H NMR (500 MHz, CD_3OD) δ: 5.79 (d, $J_{1,2}$ = 2.8 Hz, 1H, H-1), 5.42–5.39 (m, 1H, H-4), 5.10 (dd, $J_{3,2}$ = 11.7 Hz, $J_{3,4}$ = 2.8 Hz, 1H, H-3), 4.55–4.50 (m, 1H, H-5), 4.28–4.23 (m, 1H, H-5′), 4.20–4.10 (m, 2H, H-6a, H-6b), 4.00–3.88 (m, 2H, CH_2, Gly), 3.71 (dd, $J_{2,1}$ = 2.8 Hz, $J_{2,3}$ = 11.7 Hz, 1H, H-2), 3.02 (m, H-4′a,), 2.84 (m, H-4′b), 2.15 (s, 3H, $COCH_3$), 2.03 (s, 3H, $COCH_3$), 2.00 (s, 3H, $COCH_3$); ^{13}C NMR (125 MHz, CD_3OD) δ: 173.1 (C_q, CO), 172.1 ($2C_q$, CO), 171.9 (C_q, CO), 171.5 (C_q, CO), 167.1 (C_q, CO), 157.0 (C_q, CO), 97.6 (CH, C-1), 97.1 (C_q), 70.1 (CH, C-5), 68.7 (CH, C-4), 67.2 (CH, C-3), 62.8 (CH_2, C-6), 53.4 (CH, C-5′), 42.3 (CH_2, Gly), 37.4 (CH, C-2), 31.8 (CH_2, C-4′), 20.5–20.4 ($3CH_3$, Ac).

Synthesis of glycosylated SiNPs

To a solution of **6** (90 mg, 0.17 mmol) in DMF (2 mL), HBTU (197 mg, 0.52 mmol), DIPEA (121 µL, 0.70 mmol) and aminopropyl-functionalized silica gel (88 mg, 1 mmol/g NH_2 loading, 40–63 µm) were added. The suspension was stirred at room temperature for 24 h, then was filtered and washed several times with DMF and CH_2Cl_2 to give acetylated glycosylated SiNPs (110 mg). A suspension of acetylated glycosylated SiNPs (75 mg) in NH_3 in MeOH 4 M (1.5 mL) was stirred at room temperature for 48 h, then was filtered and washed several times with MeOH and CH_2Cl_2 to give deacetylated glycosylated SiNPs (60 mg). GSiNPs were characterized by $\{^1H\}$-^{13}C CP MAS spectra, which also confirmed the expected deacetylation of the sugar moiety (see also Supporting Information).

References

[1] A. Varki. *Glycobiology* **27**, 3 (2017).
[2] M.-M. Wei, Y.-S. Wang, X.-S. Ye. *Med. Res. Rev*. **38**, 1003 (2018).

[3] M. Marradi, F. Chiodo, I. García, S. Penadés. *Chem. Soc. Rev*. **42**, 4728 (2013).
[4] N. M. Molino, A. K. L. Anderson, E. L. Nelson, S.-W. Wang. *ACS Nano* **7**, 9743 (2013).
[5] T. Darbre, J.-L. Reymond. *Curr. Top Med. Chem*. **8**, 1286 (2008).
[6] Q. A. Pankhurst, J. Connolly, S. K. Jones, J. Dobson. *J. Phys. D: Appl. Phys*. **36**, R167 (2003).
[7] M. Gonzalez-Burgos, A. Latorre-Sanchez, J. A. Pomposo. *Chem. Soc. Rev*. **44**, 6122 (2015).
[8] T. Ju, V. I. Otto, R. D. Cummings. *Angew. Chem. Int. Ed. Engl*. **50**, 1770 (2011).
[9] F. Corzana, J. H. Busto, G. Jiménez-Osés, M. García de Luis, J. L. Asensio, J. Jiménez-Barbero, J. M. Peregrina, A. Avenoza. *J. Am. Chem. Soc*. **129**, 9458 (2007).
[10] A. Ardá, R. Bosco, J. Sastre, F. J. Cañada, S. André, H.-J. Gabius, B. Richichi, J. Jiménez-Barbero, C. Nativi. *Eur. J. Org. Chem*. **2015**, 6823 (2015).
[11] B. Richichi, B. Thomas, M. Fiore, R. Bosco, H. Qureshi, C. Nativi, O. Renaudet, L. BenMohamed. *Angew. Chem. Int. Ed. Engl*. **53**, 11917 (2014).
[12] M. Manuelli, S. Fallarini, G. Lombardi, C. Sangregorio, C. Nativi, B. Richichi. *Nanoscale* **6**, 7643 (2014).
[13] R. Gracia, M. Marradi, G. Salerno, R. Pérez-Nicado, A. Pérez-San Vicente, D. Dupin, J. Rodriguez, I. Loinaz, F. Chiodo, C. Nativi. *ACS Macro Lett*. **7**, 196 (2018).
[14] A. M. Schrand, M. F. Rahman, S. M. Hussain, J. J. Schlager, D. A. Smith, A. F. Syed. *Wiley Interdiscip Rev. Nanomed. Nanobiotechnol*. **2**, 544 (2010).
[15] C. K. Lyon, A. Prasher, A. M. Hanlon, B. T. Tuten, C. A. Tooley, P. G. Frank, E. B. Berda. *Polym. Chem*. **6**, 181 (2015).
[16] R. Gracia, M. Marradi, U. Cossío, A. Benito, A. Pérez-San Vicente, V. Gómez-Vallejo, H.-J. Grande, J. Llop, I. Loinaz. *J. Mater. Chem. B* **5**, 1143 (2017).
[17] N. Yokoigawa, N. Takeuchi, M. Toda, M. Inoue, M. Kaibori, H. Yanagida, H. Tanaka, T. Ogura, H. Takada, T. Okumura, A. H. Kwon, Y. Kamiyama, H. Nakada. *Clin. Cancer Res*. **11**, 6127 (2005).
[18] L. Chen, J. Liu, Y. Zhang, G. Zhang, Y. Kang, A. Chen, X. Feng, L. Shao. *Nanomedicine (Lond.)* **13**, 1939 (2018).
[19] M. Fragai, C. Luchinat, T. Martelli, E. Ravera, I. Sagi, I. Solomonov, Y. Udi. *Chem. Commun. (Camb.)* **50**, 421 (2014).
[20] E. Ravera, V. K. Michaelis, T.-C. Ong, E. G. Keeler, T. Martelli, M. Fragai, R. G. Griffin, C. Luchinat. *ChemPhysChem*. **16**, 2751 (2015).
[21] T. Martelli, E. Ravera, A. Louka, L. Cerofolini, M. Hafner, M. Fragai, C. F. W. Becker, C. Luchinat. *Chemistry* **22**, 425 (2015).
[22] E. Ravera, L. Cerofolini, T. Martelli, A. Louka, M. Fragai, C. Luchinat. *Sci. Rep*. **6**, 27851 (2016).
[23] S. Giuntini, L. Cerofolini, E. Ravera, M. Fragai, C. Luchinat. *Sci. Rep*. **7**, 17934 (2017).
[24] S. Giuntini, E. Balducci, L. Cerofolini, E. Ravera, M. Fragai, F. Berti, C. Luchinat. *Angew. Chem. Int. Ed. Engl*. **56**, 14997 (2017).
[25] E. Ravera, S. Ciambellotti, L. Cerofolini, T. Martelli, T. Kozyreva, C. Bernacchioni, S. Giuntini, M. Fragai, P. Turano, C. Luchinat. *Angew. Chem. Int. Ed. Engl*. **55**, 2446 (2016).
[26] L. Cerofolini, S. Giuntini, A. Carlon, E. Ravera, V. Calderone, M. Fragai, G. Parigi, C. Luchinat. *Chemistry* **25**, 1984 (2019).
[27] V. Marzaioli, J. A. Aguilar-Pimentel, I. Weichenmeier, G. Luxenhofer, M. Wiemann, R. Landsiedel, W. Wohlleben, S. Eiden, M. Mempel, H. Behrendt, C. Schmidt-Weber, J. Gutermuth, F. Alessandrini. *Int. J. Nanomedicine* **9**, 2815 (2014).

Supplementary Material: The online version of this article offers supplementary material (https://doi.org/10.1515/pac-2019-0210).